Punjab University Journal of Mathematics (2024), 56(12), 838-859
https://doi.org/10.52280/pujm.2024.56(12)04

Computation of $\mathfrak{R}_{\mathfrak{D}}\mathrm{M}$-Polynomial, Operators, and Topological Descriptors for Hex-Derived Networks

*Abdul Rauf Khan
Department of Mathematics, Faculty of Sciences, Ghazi University, Dera Ghazi Khan, 32200, Pakistan

Saad Amin Bhatti
Department of Mathematics, Faculty of Sciences, Ghazi University, Dera Ghazi Khan, 32200, Pakistan

Yilun Shang
Department of Computer and Information Sciences, Northumbria University, Newcastle NE1 8ST, UK

*Corresponding Author
khankts@gmail.com

Received:30 December, 2024 / Accepted: 20 June, 2025 / Published online: 11 August, 2025

Abstract. In this paper, we formulate a reverse degree $\mathfrak{R}_{\mathfrak{D}}\mathrm{M}$-Polynomial for graphs, along with differential operators and integral operators derived from it. Reverse degree topological indices are also calculated using the computed $\mathfrak{R}_{\mathfrak{D}}\mathrm{M}$-Polynomials. Numerical invariants known as topological descriptors ($\mathbb{TD}$'s) are essential for describing the molecular topology of a particular molecular graph. This method has been utilized to develop topological descriptors based on reverse degree. The present study analyses and computes the relevant indices for triangular and rectangular type-3 hex-derived networks. The results of this study provide researchers and academics with new insights that pave the way for further research and related discoveries.

AMS (MOS) Subject Classification Codes: 05C09; 05C10; 05C31; 05C35; 05C75; 05C90; 05C99; 47E05; 47G10; 47N50
Key Words: Hex-derived Network, Molecular Structure, Reverse Degree, $\mathfrak{R}_{\mathfrak{D}}$ M-Polynomial, Differential Operators, Integral Operators, Topological Descriptors, $\mathbb{THDN}_3$ and $\mathbb{RHDN}_3$.

1. Introduction

A fascinating multidisciplinary area that combines graph theory with the chemical sciences is called chemical graph theory [2]. Graph theory has been an essential tool for

chemists, providing information through topological descriptors or indices [26]. Chemical graphs, which give a structural depiction of chemical compounds, are frequently used to simulate molecular structures. Vertices in this chemical graph represent the atoms, and edges show the connections between them [15].

In recent years, cheminformatics, a field that connects mathematics, chemistry, and information science, has seen tremendous growth [23]. To anticipate the biological and physicochemical characteristics of chemical compounds, it facilitates the construction of quantitative structure-activity relationships (QSAR's) and quantitative structure-property relationships (QSPR's) [8]. Numerous indices, including the Wiener, Randic, Balaban, and Zagreb indices, are used to predict and evaluate the chemical and physical characteristics of chemical complexes [3].

In graph theory, it provides the source of fundamental symbols and terminology, such as d_λ, which denotes the degree of a vertex λ [12]. West et al. [24] define the degree of a vertex as the number of edges incident to the vertex λ. This degree is represented by the notation d_λ or $d(\lambda)$. $\mathbb{TD}$, which stands for topological descriptors, are analytical techniques used to study the structural properties of chemical graphs. Chemical graph structures are converted into numerical values via these descriptors, which are graph invariants. In 1947, Wiener introduced $\mathbb{TD}$ with an emphasis on trees. In his study, the usefulness of these indices (W) in relating the physical characteristics of substances such as alcohols, alkanes, and related compounds was emphasized [25].

The topological index of a chemical graph is a numerical value that helps characterize the physicochemical properties of that structure [1]. Graph-based topological indices are generally grouped into three primary categories: degree-based, distance-based, and counting-based indices [11].

In recent decades, QSPR studies of chemical structures have been extensively studied by employing the outcomes of the graphs topological indices. This also significantly impacts this area of study by contributing fruitful results [27]. This study has been enhanced by computing various networks [22]. A successful approach to conducting QSAR and QSPR investigations has been the use of a combination of topological indices and entropy measures [9]. It has been common practice to forecast the bioactivity of organic substances by using physicochemical and topological indices [13].

The edges of chemical graphs show chemical bonds or interactions, while the vertices indicate atoms or compounds. The structure of a graph is described by its topological descriptors ($\mathbb{TD}$), but certain graph features are measured by numerical graph invariants [14]. There has been a boom in studies in this area focussing on different molecular structures, since QSPR investigations are more cost-effective than experimental compound assessments [17].

In this paper, we compute reverse degree topological descriptors ($\mathbb{TD}$) for various hex-derived network configurations. The $\mathfrak{R}_{\mathfrak{D}}$M-polynomial, which extends the framework presented by Khan et al. [18], is a noteworthy addition of our work. It provides a new analytical method for assessing $\mathbb{TD}$.

2. AIMS OF THE STUDY

The primary goal of this study is to provide the $\mathfrak{R}_{\mathfrak{D}}\mathrm{M}$-polynomial, a reverse degree-based graph polynomial, in combination with differential and integral operators. These operators are used to derive topological descriptors.

3. NOVELTY IN THE STUDY

We use a novel concept of reverse degree $\mathfrak{R}_{\mathfrak{D}}\mathrm{M}$-polynomial, which serves as a foundation for deriving its differential and integral operators. These operators simplify the computation of topological descriptors associated with the reverse degree of graph vertices. To implement our approach, we generated molecular graphs for $\mathbb{THDN}_3$ and $\mathbb{RHDN}_3$, illustrated in Figure 4 and Figure 5.

4. MATERIAL AND METHODOLOGY

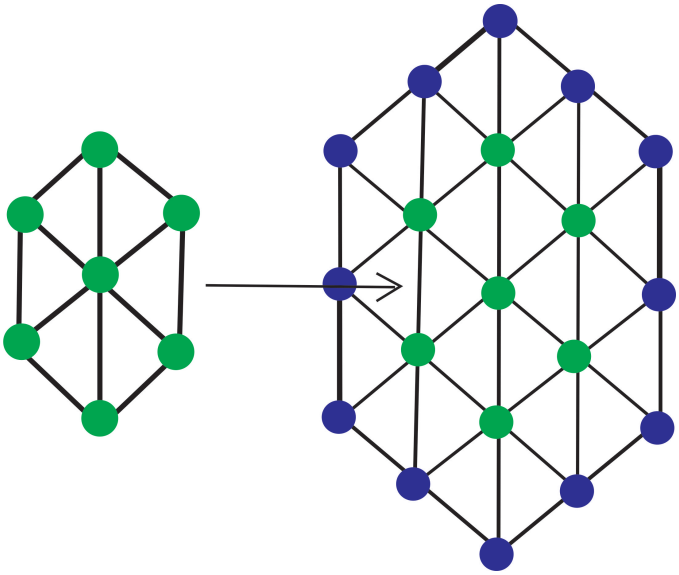

FIGURE 1. Hexagonal Meshes (a)HM_2 and (b)HM_3

4.1. **Layout of third type hexagonal-derived networks.** A hexagonal mesh can be formed by utilizing a complete graph of order 3, commonly referred to as M_3 in chemical graph theory. These M_3 graphs are widely known as oxide graphs in chemistry. When several M_3 graphs are combined, as shown in Figure 1, it results in the formation of more complex network structures. By joining six M_3 graphs, one obtains the two-dimensional mesh graph HM_2, as demonstrated in Figure 1 (a). Furthermore, placing M_3 graphs around HM generates the three-dimensional mesh graph HM_3, depicted in Figure 1 (b). This technique, first revisited by Chen et al. [7], involves enclosing each hexagon within an M_3 graph to

produce a hexagonal mesh structure. Notably, there is no known representation of a one-dimensional hexagonal mesh graph. In related work, Abbas et al. [4] studied the metric dimensions for hexagonal boron nitride, while Arnawa et al. and Fitriani et al. [5] highlighted the use of worksheet-based problems to demonstrate concepts in calculus. Balal et al. [6] provided an insightful discussion on various topological structures. Hex-derived networks, a product of the Hex algorithm, have significantly transformed the field of chemistry by aiding in the prediction of chemical interactions through machine learning models. They are crucial for enhancing protein-ligand interaction studies, speeding up the drug discovery process, and improving the virtual screening of potential compounds. These networks are invaluable tools that contribute to accelerating breakthroughs in molecular and pharmaceutical research. For computer scientists, understanding and calculating the multiplicative topological characteristics of hex-derived networks is an essential task, as it enhances the understanding of complex network topologies and facilitates the development of advanced computational algorithms.

4.2. **Algorithmic methodologies.** A simple graph is defined as one that has neither loops nor numerous edges. Chemical structures can be efficiently modelled using a basic graph $\mathcal{G}$, which is described by its vertex set $\mathcal{V}(\mathcal{G})$ and edge set $\mathcal{E}(\mathcal{G})$. The number of edges that connect to a vertex ϕ is its degree, represented by $d(\phi)$. Kulli [20] proposed the idea of a vertex's reverse degree, which is described as

$$\mathfrak{R}_{\mathfrak{D}}(\phi) = \delta(\mathcal{G}) - d(\phi) + 1,$$

where $d(\phi)$ represents the degree of vertex ϕ, $\mathfrak{R}_{\mathfrak{D}}(\phi)$ is reverse degree of the vertex $\delta(\mathcal{G})$ is the maximum degree of any vertex in the graph $\mathcal{G}$.

We consider the set $\mathfrak{R}_{\mathfrak{D}} = \{(l, m \in \mathbb{N} \times \mathbb{N}) : 1 \leq l \leq m \leq \chi\}$. For a pair of vertices ϕ and ψ with reverse degrees $\mathfrak{R}_{\mathfrak{D}}(\phi) = l$ and $\mathfrak{R}_{\mathfrak{D}}(\psi) = m$, we define $\mathfrak{R}_{\mathfrak{D}}(l, m) = \{\phi\psi \in \mathfrak{E}(\mathcal{G}) : \mathfrak{R}_{\mathfrak{D}}(\phi) = l, \mathfrak{R}_{\mathfrak{D}}(\psi) = m\}$.

Deutsch and Klavzar first proposed the idea of the M-Polynomial in 2014 [10]. The closed-form structure of several degree-based topological indices can be found using this polynomial [21]. M-Polynomial is recently studied by Khan et al. [19] . Building on this concept, we introduced a novel notion of a polynomial, namely, a reverse degree-based $\mathfrak{R}_{\mathfrak{D}}$M-Polynomial, which was previously introduced by Hakami et al. [16] as follows:

$$\mathfrak{R}_{\mathfrak{D}}\,\mathrm{M}(\mathcal{G}; \nu, \kappa) = \sum_{l \leq m} \mu_{(l,m)} \nu^l \kappa^m,$$

where ν and κ are variables corresponding to the earlier studies on M-Polynomials [16], and $\mu_{(l,m)}$ counts the number of edges $\phi\psi \in \mathfrak{E}(\mathcal{G})$ such that $\{\mathfrak{R}_{\mathfrak{D}}(\phi), \mathfrak{R}_{\mathfrak{D}}(\psi)\} = \{l, m\}$.

The formulas connecting the $\mathfrak{R}_{\mathfrak{D}}$M-Polynomial to the $\mathfrak{R}_{\mathfrak{D}}$ topological descriptors are given in Table 1.

The operators in Table 1 are defined as follows

Topological index	**Formula From** $\mathfrak{R}_{\mathfrak{D}}\mathrm{M}(\mathcal{G})$
$\mathfrak{R}_{\mathfrak{D}}M_1$	$(\mathbb{D}_\nu+\mathbb{D}_\kappa)(\mathfrak{R}_{\mathfrak{D}}\,\mathrm{M}(\mathcal{G}))\big\vert_{\nu=\kappa=1}$
$\mathfrak{R}_{\mathfrak{D}}M_2$	$(\mathbb{D}_\nu\mathbb{D}_\kappa)(\mathfrak{R}_{\mathfrak{D}}\,\mathrm{M}(\mathcal{G})\big\vert_{\nu=\kappa=1}$
$\mathfrak{R}_{\mathfrak{D}}F$	$(\mathbb{D}_\nu^2+\mathbb{D}_\kappa^2)(\mathfrak{R}_{\mathfrak{D}}\,\mathrm{M}(\mathcal{G})\big\vert_{\nu=\kappa=1}$
$\mathfrak{R}_{\mathfrak{D}}HM_1$	$(\mathbb{D}_\nu+\mathbb{D}_\kappa)^2(\mathfrak{R}_{\mathfrak{D}}\,\mathrm{M}(\mathcal{G})\big\vert_{\nu=\kappa=1}$
$\mathfrak{R}_{\mathfrak{D}}HM_2$	$(\mathbb{D}_\nu\mathbb{D}_\kappa)^2(\mathfrak{R}_{\mathfrak{D}}\,\mathrm{M}(\mathcal{G})\big\vert_{\nu=\kappa=1}$
$\mathfrak{R}_{\mathfrak{D}}\sigma$	$(\mathbb{D}_\nu-\mathbb{D}_\kappa)^2(\mathfrak{R}_{\mathfrak{D}}\,\mathrm{M}(\mathcal{G}))\big\vert_{\nu=\kappa=1}$
$\mathfrak{R}_{\mathfrak{D}}{}^mM_2$	$(\mathbb{I}_\nu\mathbb{I}_\kappa)(\mathfrak{R}_{\mathfrak{D}}\,\mathrm{M}(\mathcal{G})\big\vert_{\nu=\kappa=1}$
$\mathfrak{R}_{\mathfrak{D}}ReZG_3$	$(\mathbb{D}_\nu\mathbb{D}_\kappa)(\mathbb{D}_\nu+\mathbb{D}_\kappa)(\mathfrak{R}_{\mathfrak{D}}\,\mathrm{M}(\mathcal{G})\big\vert_{\nu=\kappa=1}$
$\mathfrak{R}_{\mathfrak{D}}SDD$	$(\mathbb{D}_\nu\mathbb{I}_\kappa+\mathbb{I}_\nu\mathbb{D}_\kappa)(\mathfrak{R}_{\mathfrak{D}}\,\mathrm{M}(\mathcal{G})\big\vert_{\nu=\kappa=1}$
$\mathfrak{R}_{\mathfrak{D}}H$	$2J\mathbb{I}_\nu(\mathfrak{R}_{\mathfrak{D}}\,\mathrm{M}(\mathcal{G})\big\vert_{\nu=\kappa=1}$
$\mathfrak{R}_{\mathfrak{D}}I$	$\mathbb{I}_\nu J\mathbb{D}_\nu\mathbb{D}_\kappa(\mathfrak{R}_{\mathfrak{D}}\,\mathrm{M}(\mathcal{G})\big\vert_{\nu=\kappa=1}$
$\mathfrak{R}_{\mathfrak{D}}A$	$I_\nu^3Q_{-2}J\mathbb{D}_\nu^3\mathbb{D}_\kappa^3(\mathfrak{R}_{\mathfrak{D}}\,\mathrm{M}(\mathcal{G})\big\vert_{\nu=\kappa=1}$

TABLE 1. Formula for deriving topological descriptors from $\mathfrak{R}_{\mathfrak{D}}$M-Polynomial

$$\mathbb{D}_\nu = \nu\frac{\partial(\mathfrak{R}_{\mathfrak{D}}\,\mathrm{M}(\mathcal{G};\nu,\kappa))}{\partial\nu} \quad (4.\ 1)$$

$$\mathbb{D}_\kappa = \kappa\frac{\partial(\mathfrak{R}_{\mathfrak{D}}\,\mathrm{M}(\mathcal{G};\nu,\kappa))}{\partial\kappa} \quad (4.\ 2)$$

$$\mathbb{I}_\nu = \int_0^\nu \frac{1}{z}(\mathfrak{R}_{\mathfrak{D}}\,\mathrm{M}(\mathcal{G};z,\kappa))dz \quad (4.\ 3)$$

$$\mathbb{I}_\kappa = \int_0^\kappa \frac{1}{z}(M(\mathcal{G};\nu,z))dz \quad (4.\ 4)$$

$$J(g(\nu,\kappa)) = g(\nu,\nu) \quad (4.\ 5)$$

$$Q_\alpha = \nu^\alpha g(\nu,\kappa) \quad (4.\ 6)$$

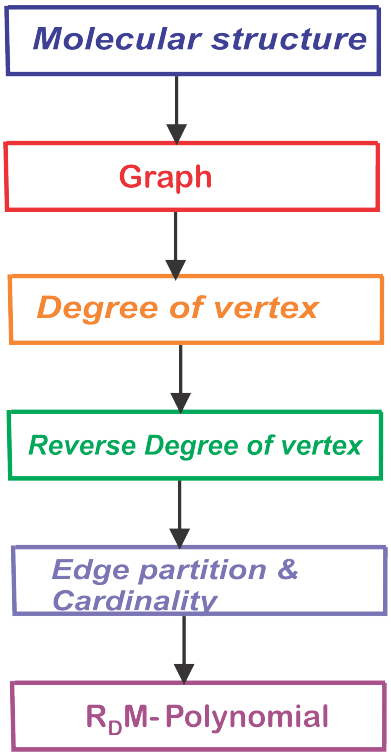

FIGURE 2. Flow Chart for computation of $\mathfrak{R}_{\mathfrak{D}}$M-Polynomial

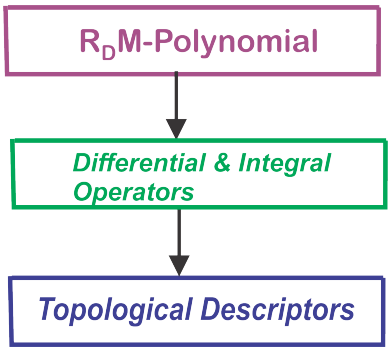

FIGURE 3. Flow Chart for computation of Topological Descriptors

5. RESULTS

This section presents the findings of the study, beginning with the derivation of analytical formulas for various reverse degree-based topological descriptors associated with different Hex-derived network structures. Figures 4-5 illustrate the structures of the hex-derived networks of interest. We adopt the notation $\mathbb{HDN}_3$ to represent hex-derived networks, $\mathbb{THDN}_3$ for triangular type-3 hex-derived network structures, and $\mathbb{RHDN}_3$ for rectangular type-3 hex-derived network structures.

5.1. **Triangular Type-3 Hex-Derived Network ($\mathbb{THDN}_3$).**

Consider $\mathbb{THDN}_3$ as the third variation of the triangular hex-derived network with a dimension of $n \geq 4$. The network $\mathbb{THDN}_3$, formed by a hexagon and arranged in a triangular shape, is illustrated in Figure 5. The edges of this network are categorized into six groups based on the degree of the vertices at each end. The Reverse degree-based edge division of the triangular type-3 hex-derived network is described in Table 2, using Figure 4.

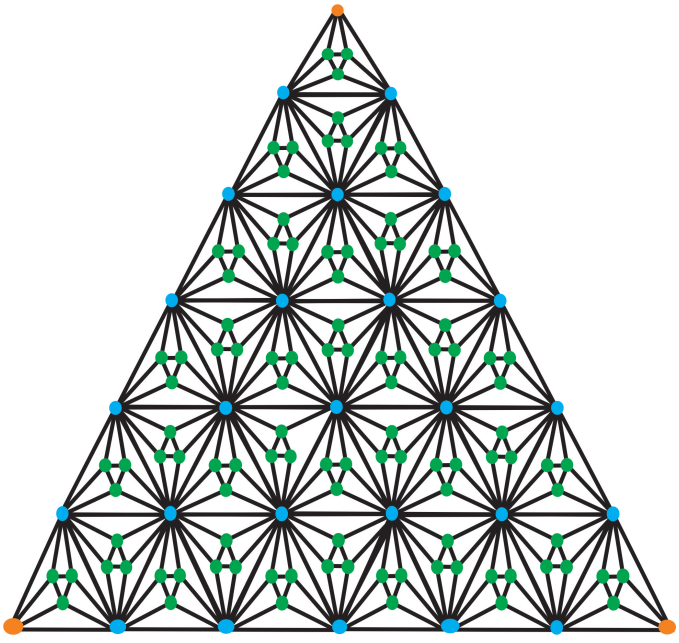

FIGURE 4. Structure of $\mathbb{THDN}_3$

$\mathfrak{R}_{\mathfrak{D}}\mathfrak{E}_{(\lambda,\tau)}$	Cardinality
$\mathfrak{E}_{(15,15)}$	$(3r^2-6r+9)$
$\mathfrak{E}_{(15,9)}$	$(18r-30)$
$\mathfrak{E}_{(15,1)}$	$(6r^2-30r+36)$
$\mathfrak{E}_{(9,9)}$	$(3r-6)$
$\mathfrak{E}_{(9,1)}$	$(6r-18)$
$\mathfrak{E}_{(1,1)}$	$(\frac{3}{2}r^2-\frac{21}{2}r+18)$

TABLE 2. $\mathfrak{R}_{\mathfrak{D}}$ edge division of $\mathbb{THDN}_3$

$\mathfrak{R}_{\mathfrak{D}}$M-Polynomial for $\mathbb{THDN}_3$

Let $\mathbb{THDN}_3$ represent the graph of a triangular type-3 hex-derived network. Let $\mathfrak{R}_{\mathfrak{D}}(l,m)$ denote the collection of all edges characterized by the reverse degree of their end vertices ν and κ, and $\mu_{l,m}$ denote the count of edges in $\mathfrak{R}_{\mathfrak{D}}(l,m)$.

$\mathfrak{R}_{\mathfrak{D}}(l,m) = \{\phi\psi \in \mathfrak{E}(\mathcal{G}) :\ \mathfrak{R}_{\mathfrak{D}}(\phi) = l,\ \mathfrak{R}_{\mathfrak{D}}(\psi) = m\}$
$\mathfrak{R}_{\mathfrak{D}}(15,15) = \{\phi\psi \in \mathfrak{E}(\mathcal{G}) :\ \mathfrak{R}_{\mathfrak{D}}(\phi) = 15,\ \mathfrak{R}_{\mathfrak{D}}(\psi) = 15\}$
$\mathfrak{R}_{\mathfrak{D}}(15,9) = \{\phi\psi \in \mathfrak{E}(\mathcal{G}) :\ \mathfrak{R}_{\mathfrak{D}}(\phi) = 15,\ \mathfrak{R}_{\mathfrak{D}}(\psi) = 9\}$
$\mathfrak{R}_{\mathfrak{D}}(15,1) = \{\phi\psi \in \mathfrak{E}(\mathcal{G}) :\ \mathfrak{R}_{\mathfrak{D}}(\phi) = 15,\ \mathfrak{R}_{\mathfrak{D}}(\psi) = 11\}$
$\mathfrak{R}_{\mathfrak{D}}(9,9) = \{\phi\psi \in \mathfrak{E}(\mathcal{G}) :\ \mathfrak{R}_{\mathfrak{D}}(\phi) = 9,\ \mathfrak{R}_{\mathfrak{D}}(\psi) = 9\}$
$\mathfrak{R}_{\mathfrak{D}}(9,1) = \{\phi\psi \in \mathfrak{E}(\mathcal{G}) :\ \mathfrak{R}_{\mathfrak{D}}(\phi) = 9,\ \mathfrak{R}_{\mathfrak{D}}(\psi) = 1\}$
$\mathfrak{R}_{\mathfrak{D}}(1,1) = \{\phi\psi \in \mathfrak{E}(\mathcal{G}) :\ \mathfrak{R}_{\mathfrak{D}}(\phi) = 1,\ \mathfrak{R}_{\mathfrak{D}}(\psi) = 1\}$

From Figure 4 and Table 2, it is clear that
$\mu_{(15,15)} = (3r^2-6r+9)$, $\mu_{(15,9)} = (18r-30)$, $\mu_{(15,1)} = (6r^2-30r+36)$, $\mu_{(9,9)} = (3r-6)$,
$\mu_{(9,1)} = (6r-18)$, $\mu_{(1,1)} = (\frac{3}{2}r^2 - \frac{21}{2}r + 18)$

The $\mathfrak{R}_{\mathfrak{D}}$M-Polynomial of $\mathbb{HDN}_3$ is computed as follow

$$\begin{aligned}\mathfrak{R}_{\mathfrak{D}}\,\mathrm{M}(\mathbb{THDN}_3) &= \sum_{l\le m}\mu_{(l,m)}\nu^l\kappa^m \\ &= \mu_{(15,15)}\nu^{15}\kappa^{15} + \mu_{(15,9)}\nu^{15}\kappa^9 + \mu_{(15,1)}\nu^{15}\kappa^1 + \mu_{(9,9)}\nu^9\kappa^9 + \mu_{(9,1)}\nu^9\kappa^1 + \mu_{(1,1)}\nu^1\kappa^1\end{aligned}$$

Putting values of $\mu_{(l,m)}$, we get

$$\begin{aligned}\mathfrak{R}_{\mathfrak{D}}\,\mathrm{M}(\mathbb{THDN}_3;\nu,\kappa) &= (3r^2-6r+9)\nu^{15}\kappa^{15} + (18r-30)\nu^{15}\kappa^9 + (6r^2-30r+36)\nu^{15}\kappa^1 \\ &+ (3r-6)\nu^9\kappa^9 + (6r-18)\nu^9\kappa^1 + (\frac{3}{2}r^2 - \frac{21}{2}r + 18)\nu^1\kappa^1 \qquad (5.\ 7)\end{aligned}$$

- The differential operators for $\mathbb{THDN}_3$

Employing Table 1 with operators (4. 1) and (4. 2) on equation (5. 7), we get

$$\begin{aligned}\mathbb{D}_\nu(\mathfrak{R}_{\mathfrak{D}}\,\mathrm{M}(\mathbb{THDN}_3;\nu,\kappa)) &= (45r^2-90r+135)\nu^{15}\kappa^{15} + (270r-450)\nu^{15}\kappa^9 + (90r^2-450r+540)\nu^{15}\kappa^1 \\ &+ (27r-54)\nu^9\kappa^9 + (54r-162)\nu^9\kappa^1 + (\frac{3}{2}r^2 - \frac{21}{2}r + 18)\nu^1\kappa^1 \qquad (5.\ 8)\end{aligned}$$

and

$$\begin{aligned}\mathbb{D}_\kappa(\mathfrak{R}_{\mathfrak{D}}\,\mathrm{M}(\mathbb{THDN}_3;\nu,\kappa)) &= (45r^2-90r+135)\nu^{15}\kappa^{15} + (18r-30)\nu^{15}\kappa^9 + (6r^2-30r+36)\nu^{15}\kappa^1 \\ &+ (27r-54)\nu^9\kappa^9 + (6r-18)\nu^9\kappa^1 + (\frac{3}{2}r^2 - \frac{21}{2}r + 18)\nu^1\kappa^1 \qquad (5.\ 9)\end{aligned}$$

- The integral operators for $\mathbb{THDN}_3$

Employing Table 1 with operators (4. 3) and (4. 4) on equation (5. 7), we get

$$\begin{aligned}\mathbb{I}_{\nu}(\mathfrak{R}_{\mathfrak{D}}\,\mathrm{M}(\mathbb{THDN}_3;\nu,\kappa)) &= \frac{1}{15}(3r^2-6r+9)\nu^{15}\kappa^{15}+\frac{1}{15}(18r-30)\nu^{15}\kappa^{9}+\frac{1}{15}(6r^2-30r+36)\nu^{15}\kappa^{1}\\ &+ \frac{1}{9}(3r-6)\nu^{9}\kappa^{9}+\frac{1}{9}(6r-18)\nu^{9}\kappa^{1}+(\frac{3}{2}r^2-\frac{21}{2}r+18)\nu^{1}\kappa^{1} \qquad (5.\ 10)\end{aligned}$$

and

$$\begin{aligned}\mathbb{I}_{\kappa}(\mathfrak{R}_{\mathfrak{D}}\,\mathrm{M}(\mathbb{THDN}_3;\nu,\kappa)) &= \frac{1}{15}(3r^2-6r+9)\nu^{15}\kappa^{15}+\frac{1}{9}(18r-30)\nu^{15}\kappa^{9}+(6r^2-30r+36)\nu^{15}\kappa^{1}\\ &+ \frac{1}{9}(3r-6)\nu^{9}\kappa^{9}+(6r-18)\nu^{9}\kappa^{1}+(\frac{3}{2}r^2-\frac{21}{2}r+18)\nu^{1}\kappa^{1} \qquad (5.\ 11)\end{aligned}$$

- **Topological Indices of $\mathbb{THDN}_3$ using $\mathfrak{R}_{\mathfrak{D}}$M-Polynomial**

Reverse 1^{st} Zagreb Index of $\mathbb{THDN}_3$

Considering Table 1, the addition of equation (5. 8) and equation (5. 9) yields

$$\begin{aligned}\mathfrak{R}_{\mathfrak{D}}M_1(\mathbb{THDN}_3) &= (\mathbb{D}_{\nu}+\mathbb{D}_{\kappa})(\mathfrak{R}_{\mathfrak{D}}\,\mathrm{M}(\mathbb{THDN}_3;\nu,\kappa))\big|_{\nu=\kappa=1}\\ \mathfrak{R}_{\mathfrak{D}}M_1(\mathbb{THDN}_3) &= 189r^2-135r-126\end{aligned}$$

Reverse 2^{nd} Zagreb Index of $\mathbb{THDN}_3$

Apply differential operator on equation (5. 9) alongwith Table 1 at $\nu=\kappa=1$, we have

$$\begin{aligned}\mathfrak{R}_{\mathfrak{D}}M_2(\mathbb{THDN}_3) &= (\mathbb{D}_{\nu}\mathbb{D}_{\kappa})(\mathfrak{R}_{\mathfrak{D}}\,\mathrm{M}(\mathbb{THDN}_3;\nu,\kappa))\big|_{\nu=\kappa=1}\\ \mathfrak{R}_{\mathfrak{D}}M_2(\mathbb{THDN}_3) &= \frac{1533}{2}r^2+\frac{1833}{2}r-2115\end{aligned}$$

Reverse Forgotten Index of $\mathbb{THDN}_3$

Considering Table 1, apply differential operators to equations (5. 8) and (5. 9), and upon adding at $\nu=\kappa=1$, we obtain

$$\begin{aligned}\mathfrak{R}_{\mathfrak{D}}F(\mathbb{THDN}_3) &= (\mathbb{D}_{\nu}^2+\mathbb{D}_{\kappa}^2)(\mathfrak{R}_{\mathfrak{D}}\,\mathrm{M}(\mathbb{THDN}_3;\nu,\kappa))\big|_{\nu=\kappa=1}\\ \mathfrak{R}_{\mathfrak{D}}F(\mathbb{THDN}_3) &= 2709r^2-3015r+594\end{aligned}$$

Reverse Hyper 1^{st} Zagreb Index of $\mathbb{THDN}_3$

Employing differential operator on equation (5. 8) and equation (5. 9) along with Table 1 at $\nu=\kappa=1$, we get

$$\begin{aligned}\mathfrak{R}_{\mathfrak{D}}HM_1(\mathbb{THDN}_3) &= (\mathbb{D}_{\nu}+\mathbb{D}_{\kappa})^2(\mathfrak{R}_{\mathfrak{D}}\,\mathrm{M}(\mathbb{THDN}_3;\nu,\kappa))\big|_{\nu=\kappa=1}\\ \mathfrak{R}_{\mathfrak{D}}HM_1(\mathbb{THDN}_3) &= 4242r^2-1182r-3636\end{aligned}$$

Reduced Hyper 2^{nd} Zagreb Index of $\mathbb{THDN}_3$

Employing differential operator $\mathbb{D}_{\nu}^2$ on equation (5. 9) along with Table 1 at $\nu=\kappa=1$, we get

$$\begin{aligned}\mathfrak{R}_{\mathfrak{D}}HM_2(\mathbb{THDN}_3) &= (\mathbb{D}_{\nu}^2\mathbb{D}_{\kappa}^2)(\mathfrak{R}_{\mathfrak{D}}\,\mathrm{M}(\mathbb{THDN}_3;\nu,\kappa))\big|_{\nu=\kappa=1}\\ \mathfrak{R}_{\mathfrak{D}}HM_2(\mathbb{THDN}_3) &= \frac{306453}{2}r^2+\frac{75417}{2}r-123831\end{aligned}$$

Reverse Sigma Index of $\mathbb{THDN}_3$
Employing differential operator on equation (5. 8) and equation (5. 9) along with Table 1 at $\nu = \kappa = 1$ and after some simplification, we get

$$\begin{aligned}\mathfrak{R}_{\mathfrak{D}}\,\sigma(\mathbb{THDN}_3) &= (\mathbb{D}_\nu - \mathbb{D}_\kappa)^2(\mathfrak{R}_{\mathfrak{D}}\,\mathrm{M}(\mathbb{THDN}_3;\nu,\kappa))\big|_{\nu=\kappa=1}\\ \mathfrak{R}_{\mathfrak{D}}\,\sigma(\mathbb{THDN}_3) &= 1176r^2 - 4848r + 4824\end{aligned}$$

Reverse Second Modified Zagreb Index of $\mathbb{THDN}_3$
By applying Integral operators on equation (5. 11) along with Table 1 at $\nu = \kappa = 1$

$$\begin{aligned}\mathfrak{R}_{\mathfrak{D}}\,{}^{m}M_2(\mathbb{THDN}_3) &= (\mathbb{I}_\nu\mathbb{I}_\kappa)(\mathfrak{R}_{\mathfrak{D}}\,\mathrm{M}(\mathbb{THDN}_3;\nu,\kappa))\big|_{\nu=\kappa=1}\\ \mathfrak{R}_{\mathfrak{D}}\,{}^{m}M_2(\mathbb{THDN}_3) &= \frac{287}{150}r^2 - \frac{15781}{1350}r + \frac{12247}{675}\end{aligned}$$

Reverse Redefined Third Zagreb Index of $\mathbb{THDN}_3$
By adding equation (5. 8) and equation (5. 9) and apply differential operators along with Table 1 at $\nu = \kappa = 1$, we get

$$\begin{aligned}\mathfrak{R}_{\mathfrak{D}}\,ReZG_3(\mathbb{THDN}_3) &= (\mathbb{D}_\nu\mathbb{D}_\kappa)(\mathbb{D}_\nu + \mathbb{D}_\kappa)(\mathfrak{R}_{\mathfrak{D}}\,\mathrm{M}(\mathbb{HDN}_3;\nu,\kappa))\big|_{\nu=\kappa=1}\\ \mathfrak{R}_{\mathfrak{D}}\,ReZG_3(\mathbb{THDN}_3) &= 21693r^2 + 15513r - 38142\end{aligned}$$

Reverse Symmetric Division Degree Index of $\mathbb{THDN}_3$
Apply differential operator (4. 1) and integral operator (4. 3) on equation (5. 9) and equation (5. 11) respectively along with Table 1 at $\nu = \kappa = 1$, we have

$$\begin{aligned}\mathfrak{R}_{\mathfrak{D}}\,SDD(\mathbb{THDN}_3) &= (\mathbb{D}_\nu\mathbb{I}_\kappa + \mathbb{I}_\nu\mathbb{D}_\kappa)(\mathfrak{R}_{\mathfrak{D}}\,\mathrm{M}(\mathbb{THDN}_3;\nu,\kappa))\big|_{\nu=\kappa=1}\\ \mathfrak{R}_{\mathfrak{D}}\,SDD(\mathbb{THDN}_3) &= \frac{497}{5}r^2 - \frac{5753}{15}r + \frac{1762}{5}\end{aligned}$$

Reverse Harmonic Index of $\mathbb{THDN}_3$
Apply operator (4. 6) on equation (5. 7) then operating integral operator $\mathbb{I}_\nu$ (4. 3) along with Table 1 at $\nu = \kappa = 1$, we have

$$\begin{aligned}\mathfrak{R}_{\mathfrak{D}}\,H(\mathbb{THDN}_3) &= 2\mathbb{I}_\nu J\mathfrak{R}_{\mathfrak{D}}\,\mathrm{M}(\mathbb{THDN}_3;\nu,\kappa)\big|_{\nu=\kappa=1}\\ \mathfrak{R}_{\mathfrak{D}}\,H(\mathbb{THDN}_3) &= \frac{49\,r^2}{20} - \frac{697\,r}{60} + \frac{49}{3}\end{aligned}$$

Reverse Inverse Sum Index of $\mathbb{THDN}_3$
Apply differential operator $\mathbb{D}_\nu$(4. 1) on equation (5. 9) then operating integral operator $\mathbb{I}_\nu$(4. 3) along with Table 1 at $\nu = \kappa = 1$, we have

$$\begin{aligned}\mathfrak{R}_{\mathfrak{D}}\,I(\mathbb{THDN}_3) &= \mathbb{I}_\nu J\mathbb{D}_\nu\mathbb{D}_\kappa(\mathfrak{R}_{\mathfrak{D}}\,\mathrm{M}(\mathbb{THDN}_3;\nu,\kappa))\big|_{l=1}\\ \mathfrak{R}_{\mathfrak{D}}\,I(\mathbb{THDN}_3) &= \frac{231\,r^2}{8} + \frac{1671\,r}{40} - \frac{1017}{10}\end{aligned}$$

5.2. **Rectangular Type-3 Hex-Derived Network** $\mathbb{RHDN}_3$**.** Figure 5 illustrates the n-dimensional, type-3 rectangular hex-derived network $\mathbb{RHDN}_3$. In the rectangular hex-derived network $\mathbb{RHDN}_3$, the number of end vertices determines how the edge set is divided into nine parts. Based on Figure 5, Table 3 outlines the $\mathfrak{R}_{\mathfrak{D}}$ edge division for $\mathbb{RHDN}_3$.

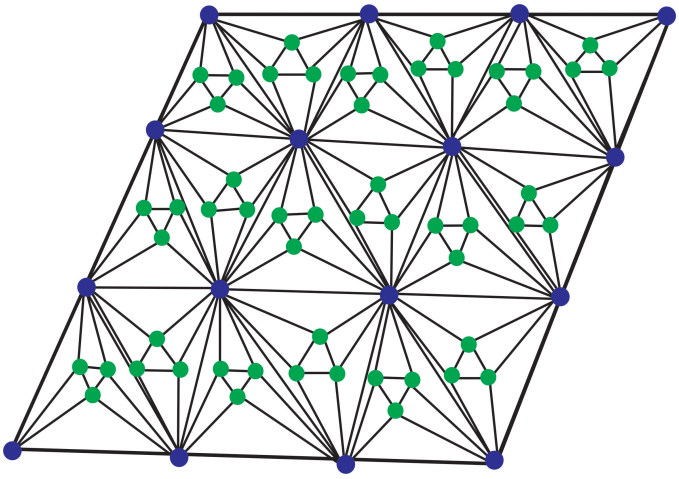

FIGURE 5. Structure of $\mathbb{RHDN}_3$

$\mathfrak{R}_{\mathfrak{D}}\mathfrak{E}_{(\lambda,\tau)}$	Cardinality
$\mathfrak{E}_{(15,15)}$	$(6r^2-12r+10)$
$\mathfrak{E}_{(15,12)}$	8
$\mathfrak{E}_{(15,9)}$	$(24r-44)$
$\mathfrak{E}_{(15,1)}$	$(12r^2-48r+48)$
$\mathfrak{E}_{(12,9)}$	4
$\mathfrak{E}_{(12,1)}$	2
$\mathfrak{E}_{(9,9)}$	$(4r-10)$
$\mathfrak{E}_{(9,1)}$	$(8r-20)$
$\mathfrak{E}_{(1,1)}$	$(3r^2-16r+21)$

TABLE 3. $\mathfrak{R}_{\mathfrak{D}}$ edge division of $\mathbb{RHDN}_3$

$\mathfrak{R}_{\mathfrak{D}}$M-Polynomial for $\mathbb{RHDN}_3$

Let $\mathbb{RHDN}_3$ be a graph of a rectangular type-3 hex-derived network. Let $\mathfrak{R}_{\mathfrak{D}}(l,m)$ denote the collection of all edges characterized by the reverse degree of their end vertices ν and κ, and $\mu_{(l,m)}$ denote the count of edges in $\mathfrak{R}_{\mathfrak{D}}(l,m)$.

$\mathfrak{R}_{\mathfrak{D}}(l,m)=\{\phi\psi\in\mathfrak{E}(\mathcal{G}):\ \mathfrak{R}_{\mathfrak{D}}(\phi)=l,\ \mathfrak{R}_{\mathfrak{D}}(\psi)=m\}$
$\mathfrak{R}_{\mathfrak{D}}(15,15)=\{\phi\psi\in\mathfrak{E}(\mathcal{G}):\ \mathfrak{R}_{\mathfrak{D}}(\phi)=15,\ \mathfrak{R}_{\mathfrak{D}}(\psi)=15\}$
$\mathfrak{R}_{\mathfrak{D}}(15,12)=\{\phi\psi\in\mathfrak{E}(\mathcal{G}):\ \mathfrak{R}_{\mathfrak{D}}(\phi)=15,\ \mathfrak{R}_{\mathfrak{D}}(\psi)=12\}$
$\mathfrak{R}_{\mathfrak{D}}(15,9)=\{\phi\psi\in\mathfrak{E}(\mathcal{G}):\ \mathfrak{R}_{\mathfrak{D}}(\phi)=15,\ \mathfrak{R}_{\mathfrak{D}}(\psi)=9\}$
$\mathfrak{R}_{\mathfrak{D}}(15,1)=\{\phi\psi\in\mathfrak{E}(\mathcal{G}):\ \mathfrak{R}_{\mathfrak{D}}(\phi)=15,\ \mathfrak{R}_{\mathfrak{D}}(\psi)=11\}$
$\mathfrak{R}_{\mathfrak{D}}(12,9)=\{\phi\psi\in\mathfrak{E}(\mathcal{G}):\ \mathfrak{R}_{\mathfrak{D}}(\phi)=12,\ \mathfrak{R}_{\mathfrak{D}}(\psi)=9\}$
$\mathfrak{R}_{\mathfrak{D}}(12,1)=\{\phi\psi\in\mathfrak{E}(\mathcal{G}):\ \mathfrak{R}_{\mathfrak{D}}(\phi)=12,\ \mathfrak{R}_{\mathfrak{D}}(\psi)=1\}$
$\mathfrak{R}_{\mathfrak{D}}(9,9)=\{\phi\psi\in\mathfrak{E}(\mathcal{G}):\ \mathfrak{R}_{\mathfrak{D}}(\phi)=9,\ \mathfrak{R}_{\mathfrak{D}}(\psi)=9\}$

$\mathfrak{R}_{\mathfrak{D}}(9,1) = \{\phi\psi \in \mathfrak{E}(\mathcal{G}) :\ \mathfrak{R}_{\mathfrak{D}}(\phi) = 9,\ \mathfrak{R}_{\mathfrak{D}}(\psi) = 1\}$
$\mathfrak{R}_{\mathfrak{D}}(1,1) = \{\phi\psi \in \mathfrak{E}(\mathcal{G}) :\ \mathfrak{R}_{\mathfrak{D}}(\phi) = 1,\ \mathfrak{R}_{\mathfrak{D}}(\psi) = 1\}$
From Figure 5 and Table 3, it is clear that

$\mu_{(15,15)} = (6r^2 - 12r + 10)$, $\mu_{(15,12)} = 8$, $\mu_{(15,9)} = (24r - 44)$, $\mu_{(15,1)} = (12r^2 - 48r + 48)$,
$\mu_{(12,9)} = 4$, $\mu_{(12,1)} = 2$, $\mu_{(9,9)} = (4r - 10)$, $\mu_{(9,1)} = (8r - 20)$, $\mu_{(1,1)} = (3r^2 - 16r + 21)$

The $\mathfrak{R}_{\mathfrak{D}}$M-Polynomial of $\mathbb{HDN}_3$ is computed as follows:

$$\mathfrak{R}_{\mathfrak{D}}\,\mathrm{M}(\mathbb{HDN}_3) \;=\; \sum_{l\leq m} \mu_{(l,m)}\nu^l\kappa^m$$

Putting values of $\mu_{(l,m)}$, we get

$$\begin{aligned}\mathfrak{R}_{\mathfrak{D}}\,\mathrm{M}(\mathbb{RHDN}_3;\nu,\kappa) &= (6r^2 - 12r + 10)\nu^{15}\kappa^{15} + 8\nu^{15}\kappa^{12} + (24r - 44)\nu^{15}\kappa^9\\ &+ (12r^2 - 48r + 48)\nu^{15}\kappa^1 + 4\nu^{12}\kappa^9 + 2\nu^{12}\kappa^1\\ &+ (4r - 10)\nu^9\kappa^9 + (8r - 20)\nu^9\kappa^1\\ &+ (3r^2 - 16r + 21)\nu^1\kappa^1 \qquad (5.\ 12)\end{aligned}$$

- The differential operators for $\mathbb{RHDN}_3$

Using Table 1 along with operators (4. 1) and (4. 2) applied on equation (5. 12), we get

$$\begin{aligned}\mathbb{D}_{\nu}(\mathfrak{R}_{\mathfrak{D}}\,\mathrm{M}(\mathbb{RHDN}_3;\nu,\kappa)) &= (90r^2 - 180r + 150)\nu^{15}\kappa^{15} + 120\nu^{15}\kappa^{12} + (360r - 660)\nu^{15}\kappa^9\\ &+ (180r^2 - 720r + 720)\nu^{15}\kappa^1 + 48\nu^{12}\kappa^9 + 24\nu^{12}\kappa^1 + (36r - 90)\nu^9\kappa^9\\ &+ (72r - 180)\nu^9\kappa^1 + (3r^2 - 16r + 21)\nu^1\kappa^1 \qquad (5.\ 13)\end{aligned}$$

and

$$\begin{aligned}\mathbb{D}_{\kappa}(\mathfrak{R}_{\mathfrak{D}}\,\mathrm{M}(\mathbb{RHDN}_3;\nu,\kappa)) &= (90r^2 - 180r + 150)\nu^{15}\kappa^{15} + 96\nu^{15}\kappa^{12} + (216r - 396)\nu^{15}\kappa^9\\ &+ (12r^2 - 48r + 48)\nu^{15}\kappa^1 + 36\nu^{12}\kappa^9 + 2\nu^{12}\kappa^1 + (36r - 90)\nu^9\kappa^9\\ &+ (8r - 20)\nu^9\kappa^1 + (3r^2 - 16r + 21)\nu^1\kappa^1 \qquad (5.\ 14)\end{aligned}$$

- The integral operators for $\mathbb{RHDN}_3$

Utilizing Table 1 along with operators (4. 3) and (4. 4) applied on equation (5. 12), we get

$$\begin{aligned}\mathbb{I}_{\nu}(\mathfrak{R}_{\mathfrak{D}}\,\mathrm{M}(\mathbb{RHDN}_3;\nu,\kappa)) &= \frac{1}{15}(6r^2 - 12r + 10)\nu^{15}\kappa^{15} + \frac{8}{15}\kappa^{12}\\ &+ \frac{1}{15}(24r - 44)\nu^{15}\kappa^9 + \frac{1}{15}(12r^2 - 48r + 48)\nu^{15}\kappa^1\\ &+ \frac{1}{3}\nu^{12}\kappa^9 + \frac{1}{6}\nu^{12}\kappa^1 + \frac{1}{9}(4r - 10)\nu^9\kappa^9 + \frac{1}{9}(8r - 20)\nu^9\kappa^1\\ &+ (3r^2 - 16r + 21)\nu^1\kappa^1 \qquad (5.\ 15)\end{aligned}$$

and

$$\begin{aligned}\mathbb{I}_{\kappa}(\mathfrak{R}_{\mathfrak{D}}\,\mathrm{M}(\mathbb{RHDN}_3;\nu,\kappa)) &= \frac{1}{15}(6r^2-12r+10)\nu^{15}\kappa^{15}\\ &+ \frac{2}{3}\nu^{15}\kappa^{12}+\frac{1}{9}(24r-44)\nu^{15}\kappa^{9}+(12r^2-48r+48)\nu^{15}\kappa^{1}\\ &+ \frac{4}{9}\nu^{12}\kappa^{9}+2\nu^{12}\kappa^{1}+\frac{1}{9}(4r-10)\nu^{9}\kappa^{9}\\ &+ (8r-20)\nu^{9}\kappa^{1}+(3r^2-16r+21)\nu^{1}\kappa^{1} \qquad (5.\ 16)\end{aligned}$$

- **Topological Indices of $\mathbb{RHDN}_3$ using $\mathfrak{R}_{\mathfrak{D}}$M-Polynomial**

Reverse First Zagreb Index of $\mathbb{RHDN}_3$

Adding equation (5. 13) and equation (5. 14) along with Table 1 at $\nu=\kappa=1$, we get

$$\begin{aligned}\mathfrak{R}_{\mathfrak{D}}M_1(\mathbb{RHDN}_3) &= (\mathbb{D}_{\nu}+\mathbb{D}_{\kappa})(\mathfrak{R}_{\mathfrak{D}}\,\mathrm{M}(\mathbb{RHDN}_3;\nu,\kappa))\big|_{\nu=\kappa=1}\\ \mathfrak{R}_{\mathfrak{D}}M_1(\mathbb{RHDN}_3) &= 378r^2-432r\end{aligned}$$

Reverse Second Zagreb Index of $\mathbb{RHDN}_3$

Apply differential operator on equation (5. 14) in view of Table 1 at $\nu=\kappa=1$, we get

$$\begin{aligned}\mathfrak{R}_{\mathfrak{D}}M_2(\mathbb{RHDN}_3) &= (\mathbb{D}_{\nu}\mathbb{D}_{\kappa})(\mathfrak{R}_{\mathfrak{D}}\,\mathrm{M}(\mathbb{RHDN}_3;\nu,\kappa))\big|_{\nu=\kappa=1}\\ \mathfrak{R}_{\mathfrak{D}}M_2(\mathbb{RHDN}_3) &= 1533r^2+200r-2043\end{aligned}$$

Reverse Forgotten Index of $\mathbb{RHDN}_3$

In view of Table 1 apply differential operators on equation (5. 13) and (5. 14) and after adding at $\nu=\kappa=1$, we have

$$\begin{aligned}\mathfrak{R}_{\mathfrak{D}}F(\mathbb{RHDN}_3) &= (\mathbb{D}_{\nu}^2+\mathbb{D}_{\kappa}^2)(\mathfrak{R}_{\mathfrak{D}}\,\mathrm{M}(\mathbb{RHDN}_3;\nu,\kappa))\big|_{\nu=\kappa=1}\\ \mathfrak{R}_{\mathfrak{D}}F(\mathbb{RHDN}_3) &= 5418r^2-7632r+2808\end{aligned}$$

Reverse Hyper 1^{st} Zagreb Index of $\mathbb{RHDN}_3$

Applying differential operator on equation (5. 13) and equation (5. 14) along with Table 1 at $\nu=\kappa=1$ and after some simplification, we have

$$\begin{aligned}\mathfrak{R}_{\mathfrak{D}}HM_1(\mathbb{RHDN}_3) &= (\mathbb{D}_{\nu}+\mathbb{D}_{\kappa})^2(\mathbb{RHDN}_3;\nu,\kappa))\big|_{\nu=\kappa=1}\\ \mathfrak{R}_{\mathfrak{D}}HM_1(\mathbb{RHDN}_3) &= 8484r^2-7232r-1278\end{aligned}$$

Reduced Hyper 2^{nd} Zagreb Index of $\mathbb{RHDN}_3$

After applying differential operator $\mathbb{D}_{\nu}^2$ on equation (5. 14) along with Table 1 at $\nu=\kappa=1$, we get

$$\begin{aligned}\mathfrak{R}_{\mathfrak{D}}HM_2(\mathbb{RHDN}_3) &= (\mathbb{D}_{\nu}^2\mathbb{D}_{\kappa}^2)(\mathfrak{R}_{\mathfrak{D}}\,\mathrm{M}(\mathbb{RHDN}_3;\nu,\kappa))\big|_{\nu=\kappa=1}\\ \mathfrak{R}_{\mathfrak{D}}HM_2(\mathbb{RHDN}_3) &= 306453r^2-154024r-45915\end{aligned}$$

Reverse Sigma Index of $\mathbb{RHDN}_3$

Applying differential operator on equation (5. 13) and equation (5. 14) along with Table 1 at $\nu=\kappa=1$ and after some simplification, we have

$$\begin{aligned}\mathfrak{R}_{\mathfrak{D}}\,\sigma(\mathbb{RHDN}_3) &= (\mathbb{D}_{\nu}-\mathbb{D}_{\kappa})^2(\mathfrak{R}_{\mathfrak{D}}\,\mathrm{M}(\mathbb{RHDN}_3;\nu,\kappa))\big|_{\nu=\kappa=1}\\ \mathfrak{R}_{\mathfrak{D}}\,\sigma(\mathbb{RHDN}_3) &= 2352r^2-8032r+6894\end{aligned}$$

Reverse Second Modified Zagreb of $\mathbb{RHDN}_3$
By applying Integral operators on equation (5. 16) along with Table 1 at $\nu = \kappa = 1$

$$\begin{aligned} \mathfrak{R}_{\mathfrak{D}}\, {}^{m}M_2(\mathbb{RHDN}_3) &= (\mathbb{I}_\nu \mathbb{I}_\kappa)(\mathfrak{R}_{\mathfrak{D}}\, \mathrm{M}(\mathbb{RHDN}_3; \nu, \kappa))\big|_{\nu=\kappa=1} \\ \mathfrak{R}_{\mathfrak{D}}\, {}^{m}M_2(\mathbb{RHDN}_3) &= \frac{287\, r^2}{75} - \frac{36728\, r}{2025} + \frac{3535}{162} \end{aligned}$$

Reverse Redefined Third Zagreb Index of $\mathbb{RHDN}_3$
By adding equation (5. 13) and equation (5. 14) and apply differential operators along with Table 1 at $\nu = \kappa = 1$, we get

$$\begin{aligned} \mathfrak{R}_{\mathfrak{D}}\, ReZG_3(\mathbb{RHDN}_3; r, t) &= (\mathbb{D}_\nu \mathbb{D}_\kappa)(\mathbb{D}_\nu + \mathbb{D}_\kappa)(\mathfrak{R}_{\mathfrak{D}}\, \mathrm{M}(\mathbb{RHDN}_3; \nu, \kappa))\big|_{\nu=\kappa=1} \\ \mathfrak{R}_{\mathfrak{D}}\, ReZG_3(\mathbb{RHDN}_3; r, t) &= 43386r^2 - 8240r - 31614 \end{aligned}$$

Reverse Symmetric Division Degree Index of $\mathbb{RHDN}_3$
Apply differential operator (4. 1) and integral operator (4. 3) on equation (5. 12) and equation (5. 16) respectively along with Table 1 at $\nu = \kappa = 1$, we have

$$\begin{aligned} \mathfrak{R}_{\mathfrak{D}}\, SDD(\mathbb{RHDN}_3) &= (\mathbb{D}_\nu \mathbb{I}_\kappa + \mathbb{I}_\nu \mathbb{D}_\kappa)(\mathfrak{R}_{\mathfrak{D}}\, \mathrm{M}(\mathbb{RHDN}_3; \nu, \kappa))\big|_{\nu=\kappa=1} \\ \mathfrak{R}_{\mathfrak{D}}\, SDD(\mathbb{RHDN}_3) &= \frac{994\, r^2}{5} - \frac{28976\, r}{45} + \frac{47893}{90} \end{aligned}$$

Reverse Harmonic Index of $\mathbb{RHDN}_3$
Apply operator (4. 6) on equation (5. 12) then operating integral operator $\mathbb{I}_\nu$ (4. 3) along with Table 1 at $\nu = \kappa = 1$, we have

$$\begin{aligned} \mathfrak{R}_{\mathfrak{D}}\, H(\mathbb{RHDN}_3) &= 2\mathbb{I}_\nu J \mathfrak{R}_{\mathfrak{D}}\, \mathrm{M}(\mathbb{RHDN}_3; \nu, \kappa)\big|_{\nu=\kappa=1} \\ \mathfrak{R}_{\mathfrak{D}}\, H(\mathbb{RHDN}_3) &= \frac{49\, r^2}{10} - \frac{844\, r}{45} + \frac{49558}{2457} \end{aligned}$$

Reverse Inverse Sum Index of $\mathbb{RHDN}_3$
Apply differential operator $\mathbb{D}_\nu$ (4. 1) on equation (5. 14) then operating integral operator $\mathbb{I}_\nu$(4. 3) and operator (4. 6) respectively along with Table 1 at $\nu = \kappa = 1$, we have

$$\begin{aligned} \mathfrak{R}_{\mathfrak{D}}\, I(\mathbb{RHDN}_3) &= \mathbb{I}_\nu J \mathbb{D}_\nu \mathbb{D}_\kappa(\mathfrak{R}_{\mathfrak{D}}\, \mathrm{M}(\mathbb{RHDN}_3; \nu, \kappa))\big|_{l=1} \\ \mathfrak{R}_{\mathfrak{D}}\, I(\mathbb{RHDN}_3) &= \frac{231\, r^2}{4} + \frac{86\, r}{5} - \frac{28460}{273} \end{aligned}$$

6. Numerical Computation and Graphical Comparison for Hex-Derived Networks

The numerical values of $\mathfrak{R}_{\mathfrak{D}}$ based topological descriptors ($\mathbb{TD}$'s) for $\mathbb{THDN}_3$ are provided in Table 4 and Table 5. For computational reasons, we consider values of r ranging from 4 to 12. We additionally displayed a visual depiction of these numerical calculations in Figure 6. As the values of r increased, there was a progressive increase in the values of $\mathfrak{R}_{\mathfrak{D}}$ based on topological descriptors ($\mathbb{TD}$'s).

r	$\mathfrak{R}_{\mathfrak{D}}\,\mathrm{M}_1$	$\mathfrak{R}_{\mathfrak{D}}\,\mathrm{M}_2$	$\mathfrak{R}_{\mathfrak{D}}\,F$	$\mathfrak{R}_{\mathfrak{D}}\,HM_1$	$\mathfrak{R}_{\mathfrak{D}}\,HM_2$	$\mathfrak{R}_{\mathfrak{D}}\,\sigma$
4	2358	13815	31878	59508	2478627	4248
5	3924	21630	53244	96504	3895374	9984
6	5868	30978	80028	141984	5618574	18072
7	8190	41859	112230	195948	7648227	28512
8	10890	54273	149850	258396	9984333	41304
9	13968	68220	192888	329328	12626892	56448
10	17424	83700	241344	408744	15575904	73944
11	21258	100713	295218	496644	18831369	93792
12	25470	119259	354510	593028	22393287	115992

TABLE 4. Computed data of topological descriptors for $\mathbb{THDN}_3$

r	$\mathfrak{R}_{\mathfrak{D}}\,{}^{m}M_2$	$\mathfrak{R}_{\mathfrak{D}}\,ReZG_3$	$\mathfrak{R}_{\mathfrak{D}}\,SDD$	$\mathfrak{R}_{\mathfrak{D}}\,H$	$\mathfrak{R}_{\mathfrak{D}}\,I$
4	1.99	370998	408.66	9.06	527.40
5	7.528	581748	919.73	19.5	829.05
6	16.88	835884	1629.6	34.83	1188.45
7	30.07	1133406	2538.26	55.06	1605.60
8	47.08	1474314	3645.73	80.2	2080.50
9	67.92	1858608	4952	110.23	2613.15
10	92.58	2286288	6457.06	145.16	3203.55
11	121.07	2757354	8160.93	185	3851.70
12	153.38	3271806	10063.6	229.73	4557.60

TABLE 5. Computed data of topological descriptors for $\mathbb{THDN}_3$

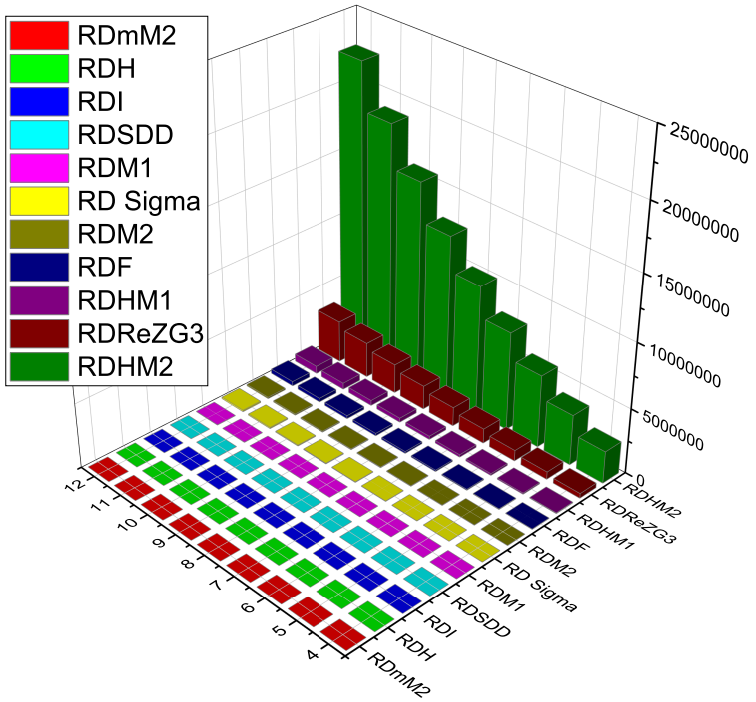

FIGURE 6. Graphical representation of Computed numerical values of $\mathcal{R}_{\mathcal{D}}\mathcal{TD}s$ of $\mathbb{THDN}_3$

The numerical values of $\mathfrak{R}_{\mathfrak{D}}$ based topological descriptors ($\mathbb{TD}$'s) for $\mathbb{RHDN}_3$ are provided in Table 6 and Table 7. For computational purposes, we considered values of r ranging from 4 to 12. A graphical depiction of these numerical values is presented in Figure 7. As the values of r increased, the values of $\mathfrak{R}_{\mathfrak{D}}$ based topological descriptors ($\mathbb{TD}$'s) increased proportionally.

r	$\mathfrak{R}_{\mathfrak{D}}\,\mathrm{M}_1$	$\mathfrak{R}_{\mathfrak{D}}\,\mathrm{M}_2$	$\mathfrak{R}_{\mathfrak{D}}\,F$	$\mathfrak{R}_{\mathfrak{D}}\,HM_1$	$\mathfrak{R}_{\mathfrak{D}}\,HM_2$	$\mathfrak{R}_{\mathfrak{D}}\,\sigma$
4	4320	23285	58968	105538	4241237	12398
5	7290	37282	100098	174662	6845290	25534
6	11016	54345	152064	260754	10062249	43374
7	15498	74474	214866	363814	13892114	65918
8	20736	97669	288504	483842	18334885	93166
9	26730	123930	372978	620838	23390562	125118
10	33480	153257	468288	774802	29059145	161774
11	40986	185650	574434	945734	35340634	203134
12	49248	221109	691416	1133634	42235029	249198

TABLE 6. Computational values of topological indices for $\mathbb{RHDN}_3$

r	$\mathfrak{R}_{\mathfrak{D}}\ {}^{m}M_2$	$\mathfrak{R}_{\mathfrak{D}}\ ReZG_3$	$\mathfrak{R}_{\mathfrak{D}}\ SDD$	$\mathfrak{R}_{\mathfrak{D}}\ H$	$\mathfrak{R}_{\mathfrak{D}}\ I$
4	10.50	629602	1137.30	23.55	888.5509
5	26.80	1011836	2282.59	48.89	1425.5009
6	50.76	1480842	3825.48	84.04	2077.9509
7	82.37	2036620	5765.97	128.98	2845.9009
8	121.63	2679170	8104.06	183.73	3729.3509
9	168.55	3408492	10839.74	248.27	4728.3009
10	223.11	4224586	13973.03	322.61	5842.75
11	285.33	5127452	17503.92	406.75	7072.70
12	355.21	6117090	21432.41	500.70	8418.15

TABLE 7. Numerical values of topological descriptors for $\mathbb{RHDN}_3$

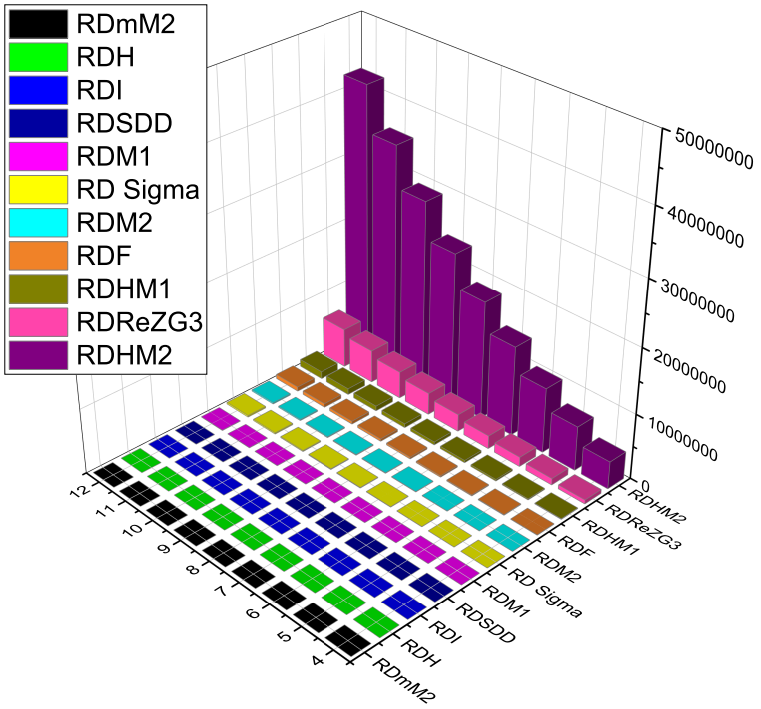

FIGURE 7. Graphical representation of Computed numerical values of $\mathcal{R}_{\mathcal{D}}\mathcal{TD}s$ of $\mathbb{RHDN}_3$

7. CONCLUSION

This paper introduces the concept of the $\mathfrak{R}_{\mathfrak{D}}$M-Polynomial, derived from the reverse degrees of a graph. From this, differential and integral operators are extracted, which facilitate the formulation of reverse degree-based $\mathbb{TD}$'s. For the structures of $\mathbb{THDN}_3$ and $\mathbb{RHDN}_3$, this study presents the corresponding $\mathfrak{R}_{\mathfrak{D}}$M-Polynomials.

$$\begin{aligned}
\mathfrak{R}_{\mathfrak{D}}\,\mathrm{M}(\mathbb{THDN}_3;\nu,\kappa) &= (3r^2-6r+9)\nu^{15}\kappa^{15}+(18r-30)\nu^{15}\kappa^{9}\\
&+ (6r^2-30r+36)\nu^{15}\kappa^{1}\\
&+ (3r-6)\nu^{9}\kappa^{9}+(6r-18)\nu^{9}\kappa^{1}\\
&+ (\frac{3}{2}r^2-\frac{21}{2}r+18)\nu^{1}\kappa^{1}\\
\mathfrak{R}_{\mathfrak{D}}\,\mathrm{M}(\mathbb{RHDN}_3;\nu,\kappa) &= (6r^2-12r+10)\nu^{15}\kappa^{15}+8\nu^{15}\kappa^{12}+(24r-44)\nu^{15}\kappa^{9}\\
&+ (12r^2-48r+48)\nu^{15}\kappa^{1}+4\nu^{12}\kappa^{9}+2\nu^{12}\kappa^{1}+(4r-10)\nu^{9}\kappa^{9}\\
&+ (8r-20)\nu^{9}\kappa^{1}+(3r^2-16r+21)\nu^{1}\kappa^{1}
\end{aligned}$$

We computed eleven topological indices, alongside differential and integral operators, using the $\mathfrak{R}_{\mathfrak{D}}$M-Polynomial. Both numerical and visual evaluations of these indices were carried out. These results are expected to inspire researchers to explore new outcomes for alternative molecular structures using this methodology.

This manuscript presents key findings regarding the eleven $\mathfrak{R}_{\mathfrak{D}}$ topological descriptors for hex-derived molecular network structures. Given the extensive nature of our findings, we provide a detailed numerical and graphical analysis of these descriptors for various initial values of the employed parameters, as shown in Tables 4-7 and Figures 6-7. Based on the results and comparisons, each calculated topological index is either a positive or negative descriptor for characterizing the three different hex-derived network structures. These descriptors are ranked hierarchically according to their values, which are determined through mathematical computations, numerical analysis, and graphical analysis. The following order of inequality shows which topological descriptor is most strongly correlated with the structure of $\mathbb{THDN}_3$ and $\mathbb{RHDN}_3$:
$\mathfrak{R}_{\mathfrak{D}}HM_2 > \mathfrak{R}_{\mathfrak{D}}ReZG_3 > \mathfrak{R}_{\mathfrak{D}}HM_1 > \mathfrak{R}_{\mathfrak{D}}F > \mathfrak{R}_{\mathfrak{D}}M_2 > \mathfrak{R}_{\mathfrak{D}}\sigma > \mathfrak{R}_{\mathfrak{D}}M_1 > \mathfrak{R}_{\mathfrak{D}}SDD > \mathfrak{R}_{\mathfrak{D}}I > \mathfrak{R}_{\mathfrak{D}}H > \mathfrak{R}_{\mathfrak{D}}{}^{m}M_2$

LIST OF ABBREVIATIONS

Abbreviation	Description
$\mathcal{R}_D$	Reverse Degree
$\mathcal{R}_D M$-Polynomial	Reverse Degree Polynomial
$\mathbb{TD}$	Topological Descriptor
$\mathbb{THDN}_3$	Triangular Type-3 Hex-Derived Network
$\mathbb{RHDN}_3$	Rectangular Type-3 Hex-Derived Network

TABLE 8. List of abbreviations

CONFLICT OF INTERESTS

The authors declare no conflicts of interest.

FUNDING

No funds, grants, or other support were received.

AUTHOR'S CONTRIBUTION

A. R. Khan: Conceptualization, Methodology, Formal Analysis, Resources, Validation, Review and Editing. S. A. Bhatti: Conceptualization, Methodology, Data Curation, Formal analysis, Writing Original Draft. Y. Shang: Conceptualization, Methodology, Formal Analysis, Validation, Writing Review and Editing. All authors read and approved the final manuscript.

REFERENCES

[1] F. Ali, B. A. Rather, M. Sarfraz, A. Ullah, N. Fatima, & W. K. Mashwani, *Certain topological indices of non-commuting graphs for finite non-abelian groups*, Molecules. **27**, No. 18 (2022) 6053.

[2] A. Ali, B. Furtula, I. Redzepovic, & I. Gutman, *Atom-bond sum-connectivity index*, J. Math. Chem. **60**, No. 10 (2022) 2081-2093.

[3] H. Ali, M. Shafiq, M. Farahani, M. Cancan, & Aldemir, M. *Degree-based topological descriptors of star of david and hexagonal cage networks*, Degree-based topological descriptors of star of david and hexagonal cage networks. **2**, (2020) 1093-1100.

[4] W. Abbas, F. Chaudhry, U. Farooq, M. Azeem, & Y. Shang, *Investigating metric dimension and edge metric dimension of hexagonal boron nitride and carbon nanotubes*, Eur. J. Pure Appl. Math. **17**, No. 3 (2024) 2055-2072.

[5] I. M. Arnawa, & N. Fitriani, *Constructing calculus concepts through worksheet based problem-based learning assisted by GeoGebra software*, HighTech Innov. J. **3**, No. 3 (2022) 282-296.

[6] A. Balal, S. Dinkhah, F. Shahabi, M. Herrera, & Y. L. Chuang, *A review on multilevel inverter topologies*, Emerg. Sci. J. **6**, No. 1 (2022) 185-200.

[7] M. S. Chen, K. G. Shin, & D. D. Kandlur, *Addressing, routing, and broadcasting in hexagonal mesh multiprocessors*, IEEE Trans. Comput. **39**, No. 1 (1990) 10-18.

[8] A. Doley, J. Buragohain, & A. Bharali, *Inverse sum indeg status index of graphs and its applications to octane isomers and benzenoid hydrocarbons*, Chemom. Intell. Lab. Syst. **203**, (2020) 104059.

[9] J. Devillers, & A. T. Balaban, *Topological indices and related descriptors in QSAR and QSPR*, Amsterdam, The Netherlands, (1999).

[10] E. Deutsch, & S. Klavzar, *M-polynomial and degree-based topological indices*, arXiv preprint arXiv: (2014) 1407.1592.
[11] M. Eliasi, & A. Iranmanesh, *On ordinary generalized geometric–arithmetic index*, Appl. Math. Lett. **24**, No. 4 (2011) 582-587.
[12] S. Edition, & K. H. Rosen, *Discrete Mathematics and Its Applications*, (2019).
[13] B. Furtula, & I. Gutman, *A forgotten topological index*, J. Math. Chem. **53**, No. 4 (2015) 1184-1190.
[14] B. Furtula, K. Ch. Das, & I. Gutman, *Comparative analysis of symmetric division deg index as potentially useful molecular descriptor*, Int. J. Quant. Chem. **118**, No. 17 (2018) e25659.
[15] M. N. Husin, R. Hasni, N. E. Arif, & M. Imran, *On topological indices of certain families of nanostar dendrimers*, Molecules. **21**, No. 7 (2016) 821.
[16] K. H. Hakami, A. R. Khan, & S. A. Bhatti, *Computation of Differential, Integral Operators and Quantitative Structure–Property Analysis of Boron α-Icosahedral Nanosheet*, J. Math. **2025**, No. 1 (2025) 5607620.
[17] S. M. Hosamani, *Correlation of domination parameters with physicochemical properties of octane isomers*, Appl. Math. Nonlinear Sci. **1**, No. 2 (2016) 345-352.
[18] A. R. Khan, S. A. Bhatti, F. Tawfiq, M. K. Siddiqui, S. Hussain, & M. A. Ali, *On degree-based operators and topological descriptors of molecular graphs and their applications to QSPR analysis of carbon derivatives*, Sci. Rep. **14**, No. 1 (2024) 21543.
[19] A. R. Khan, S. A. Bhatti, M. Imran, F. M. Tawfiq, M. Cancan, & S. Hussain, *Computation of differential and integral operators using M-polynomials of gold crystal*, Heliyon. **10**, No. 14 (2024).
[20] V. R. Kulli, *Graph indices*, Handbook of Research on Advanced Applications of Graph Theory in Modern Society, (2020) 66-91.
[21] Y. C. Kwun, M. Munir, W. Nazeer, S. Rafique, & S. M. Kang, *M-Polynomials and topological indices of V-Phenylenic Nanotubes and Nanotori*, Sci. Rep. **7**, No. 1 (2017) 8756.
[22] S. Noureen, A. Ali, A. A. Bhatti, A. M. Alanazi, & Y. Shang, *Predicting enthalpy of formation of benzenoid hydrocarbons and ordering molecular trees using general multiplicative Zagreb indices*, Heliyon. **10**, No. 10 (2024) e30913.
[23] Z. Raza, S. Akhter, & Y. Shang, *Expected value of first Zagreb connection index in random cyclooctatetraene chain, random polyphenyls chain, and random chain network*, Front. Chem. **10**, (2023) 1067874.
[24] D. B. West, *Introduction to graph theory*, **2**, 2001.
[25] H. Wiener, *Structural determination of paraffin boiling points*, J. Amer. Chem. Soc. **69**, No. 1 (1947) 17-20.
[26] V. R. Kulli, *HDR Zagreb indices of remdesivir, chloroquine, hydroxychloroquine: Research for the treatment of COVID-19*, SSRG Int. J. Appl. Chem. **9**, No. 1 (2022) 1-19.
[27] S. Zaman, W. Ahmed, A. Sakeena, K. B. Rasool, & M. A. Ashebo, *Mathematical modeling and topological graph description of dominating David derived networks based on edge partitions*, Sci. Rep. **13**, No. 1 (2023) 15159.